

Finite Element Simulation of Piezoelectric Wafer Active Sensors for Structural Health Monitoring with Coupled-Filed Elements

Weiping Liu, Victor Giurgiutiu
Department of Mechanical Engineering, Univ. of South Carolina, Columbia, SC USA 29208

ABSTRACT

Crack detection with piezoelectric wafer active sensors (PWAS) is emerging as an effective and powerful technique in structural health monitoring (SHM). Modeling and simulation of PWAS and host structure play an important role in the SHM applications with PWAS. For decades finite element method has been extensively applied in the analysis of piezoelectric materials and structures. The advantage of finite element analysis over analytical solutions is that stress and electrical field measurements of complex geometries, and their variations throughout the device, are more readily calculated. FEM allows calculation of the stress and electric field distributions under static loads and under any applied electrical frequency, and so the effect of device geometry can be assessed and optimized without the need to manufacture and test numerous devices. Coupled field analysis taking both mechanical motions and electrical characteristics into account should all be employed to provide a systemic overview of the piezoelectric sensors/actuators (even arrays of them) and the host structures.

This use of PWAS for SHM has followed two main paths: (a). Wave propagation (b). Electromechanical impedance; Previous research has shown that PWAS can detect damage using wave reflections, changes in wave signature, or changes in the electromechanical (E/M) impedance spectrum. The primary goal of this paper is to investigate the use of finite element method (FEM) to simulate various SHM methods with PWAS. For the simulation of Electro-mechanical (E/M) impedance technique, simple models, like free PWAS of different shapes and 1-dimension beam with PWAS are investigated and the simulated structural E/M impedance was presented. For the wave propagation SHM technique, a long beam with several PWAS installed was studied. One PWAS is excited by tone burst signals and elastic wave will propagate along the beam. The existence of a crack will affect the structure integrity and the echo reflected by crack can be observed through the simulations. By using the coupled field elements, direct simulation of electro-mechanical interaction of the PWAS and the host structure was made possible. The electrical potential generated on the PWAS surface by the stimulation of elastic wave can be examined in our FEM analysis. The simulation results are then compared to analytical calculation and experimental data.

Key words: Structural Health Monitoring, PWAS, finite element analysis, E/M impedance, coupled field analysis, wave propagation, Lamb wave

1. INTRODUCTION: STRUCTURAL HEALTH MONITORING (SHM) WITH PWAS

Structural health monitoring (SHM) is an emerging field with multiple applications. Structural health monitoring assets the state of structural health and, through appropriate data processing and interpretation, predicts the remaining life of the structure. The primary goal of SHM is to ascertain the existence of damage within a system being monitored. SHM sets out to determine the health of a structure by readings an array of sensors that are embedded (permanently attached) into the structure and monitored over time. In recent years, Piezoelectric Wafer Active Sensors (PWAS) has shown its potentials in active SHM applications and the use of embedded PWAS for the detection of material damage has experienced an ascending trend¹. PWAS are small and lightweight with relatively low cost. PWAS can be bonded to the structure or inserted into the layers of a composite structure. PWAS will act as active sensors, which means that it will not only sense the structure changes but also actuate the structure. When permanently attached/embedded into the structure, PWAS provide the bidirectional energy transduction from the electronics into the structure, and from the structure back into the electronics. The direct piezoelectric effect occurs when the applied stress on the sensor is converted into electric charge. The inverse effect, conversely, will produce strain when a voltage is applied on the sensor. In this way, the PWAS can be used as both, transmitter and receiver.

This use of PWAS for SHM has followed two main paths: (a) Wave propagation; (b) Electromechanical impedance. Previous research has shown that PWAS can detect damage using wave reflections (pulse-echo) method, changes in wave signature (pitch-catch method), or changes in the electromechanical (E/M) impedance spectrum¹.

The main idea of PWAS based SHM is to utilize the mechanical-electrical interactions of piezoelectric materials for the diagnosis the structural safety and health and a prognosis of the remaining life. Although the governing physical equations for the piezoelectric applications seem quite straightforward, when it comes to different host structure and situation, various difficult problems may arise. In a practical SHM system, the sensing/actuating elements, the examined structures and the driving and receiving circuits build up a coupled field system. These elementary parts of a SHM system are not isolated; they are interacting with each other in a strongly coupled way.

As for the developing of theories and applications of SHM, a deep understanding can be gained from studying and manipulating analytic expressions. Nevertheless, despite its advantage, this method is often useful only for obtaining rough approximations. A deep knowledge of the piezoelectric phenomenon is needed to set up the basic equations correctly. Also, this approach can be used only on a limited number of geometries and setup of practical applications, and approximations are often needed for this approach to be manageable.

The numerical simulation, i.e., finite element analysis (FEA) overcomes many of these drawbacks and the numerical has been extensively applied in solving practical engineering problems. Numerical simulations offer several possibilities that are not easily realized with experiments. For instance, material parameters can be manipulated and static events can be studied. The simplicity of the active geometry of micro-machined structures allows for reduced simulation times if FEA is combined with well-proven analytical expressions. The ever increasing computing power available even for common desktops and workstations already allows people to perform more realistic full-scale parametric simulations with finer meshes and less restrictive assumptions². So, to optimize the study of the Mechatronics of PWAS based SHM, numerical simulations should be combined with both analytical analysis and practical experiments, the most time-efficient approach is often to use simple analytic expressions to get a rough estimation of performance, refine it by using FEA for part of the geometry and physical effects, and combine the results in software that can handle symbolic mathematics. This approach combines the strengths of FEA and the analytic approaches by creating both a general understanding and giving accurate predictions. As always with simulations, the modeling and simulation efforts will be continuously compared with experimental results in order to validate the simulation and improve the modeling.

Various piezoelectric finite elements, in different forms such as solid, shells, plates and beams have been developed to represent the piezoelectric adaptive structures and applications. Coupled field elements, incorporating both mechanical and electrical degrees of freedoms, reflect the electro-mechanical coupling character of piezoelectric materials naturally and thus become a power tool to study the interactions of piezoelectric active sensors with host structures.

Impedance based SHM techniques have been developed as a promising method for SHM³. PZT materials have been selected as the key component for the impedance method. Wafers or patches made of PZT can be used as both actuators and sensors and their electrical impedance can be used as identifier for changes in the dynamic characteristics of host structures. A commercial impedance analyzer is usually required to collect the impedance of PZT sensors in impedance-based structural health monitoring, impedance data are first acquired while the structure is in healthy condition as pristine references. Running-time impedance data are then compared to the pristine data to identify the possible structural change.

This rest of the paper is organized as follows: In Section 2 we will introduce the electromechanical impedance technique and present the simulation results of impedance. Free square PWAS, circular PWAS and 1-D beam with square PWAS are studied. Section3 discusses the wave propagation technique with PWAS. Section 4 gives some discussions and concludes.

2. NUMERICAL SIMULATION OF ELECTROMECHANICAL (E/M) IMPEDANCE OF FREE PWAS

2.1. Electromechanical (E/M) impedance technique overview

The electro-mechanical (E/M) impedance method is an emerging technology that uses in-plane surface excitation to measure the point wise mechanical impedance of the structure through the real part of the electrical impedance measured at the sensor terminals^{4,5,6,7}. The E/M impedance technique utilizes the direct and the converse electro-mechanical properties of piezoelectric materials, allowing for the simultaneous actuation and sensing of the

structural response⁶. The variation of the electro-mechanical impedance of piezoelectric sensor-actuators (wafer transducers) intimately bonded to the structure is monitored over a large frequency spectrum in the high kHz frequency band. Their frequency response, the measured impedance parameters such as real and imaginary parts, amplitude, phase, etc. serve as potential indicators of structural damage and reflects the state of structural integrity. The method has been shown to be especially effective at ultrasonic frequencies, which properly capture the changes in local dynamics due to incipient structural damage¹. Such changes are too small to affect the global dynamics and hence cannot be readily detected by conventional low frequency vibration methods.

2.2. Numerical Electromechanical (E/M) impedance simulation of free PWAS

First we will start the impedance simulation with square and circular free PWAS. Free PWAS will be modeled with finite element coupled filed elements. Then time harmonic analyses are performed on the free PWAS to obtain the electrical charge. With the electrical charge data we can calculate the electromechanical (E/M) impedance of the PWAS, then the comparison of simulated results with experimental are provided.

In the coupled field analysis of PWAS, coupled filed elements which could deal with both mechanical and electrical fields are used to model the PWAS. The coupled field finite element we used is a 3-D brick element that has eight nodes with up to six degrees of freedom at each node. When used for piezoelectric analysis, it could have an extra electrical voltage DOF in addition to these displacement DOFs; for each DOF of a node, there is a reaction force F_X, F_Y, F_Z that corresponds to the X, Y, Z displacement DOFs respectively and charge Q corresponds to the voltage DOF. This charge Q is utilized to calculate the impedance data. For the coupled filed piezoelectric analysis, stress field and electric field are coupled together so that change in one field will induce change in the other field. Thus alternating electric voltage V can be direct applied on the coupled field elements as constrains and electrical charge will accumulate as reaction force Q , and impedance Z is calculated as V/I where I is the current value and V is the applied potential voltage. The current I comes from the accumulated charge on the electrode surface of PWAS and it is calculated as $I = j\omega\sigma Q_i$, where ω is the operating frequency, j is $\sqrt{-1}$ and ΣQ_i is the summed nodal charge (nodal reaction load). When excited by an alternating electric voltage the free PWAS acts as an electromechanical resonator. The modeling of a free PWAS is useful for the understanding the electromechanical coupling between the mechanical vibration response and the complex electrical response of the sensor.

Harmonic analysis was performed on the square and circular PWAS model to obtain the frequency response of the electrical mechanical impedance. Excitation of sinusoidal voltage was applied on the nodes at the top and bottom surface and the excitation signal will sweep a certain frequency range as the commercial impedance analyzer does. When excited by alternating voltage, electrical charge, i.e. the reaction force Q to the electrical potential was accumulated on the nodes at the surface of PWAS elements. Then the impedance Z at sensor terminals is calculated as V/I where I is the current and V is the applied potential.

Table 1 Free PWAS model

FE Model						
Shape	Thickness	Dimension	Element length	Number of elements	nodes	Materials
Square	0.2 mm	7mm × 7mm	0.25mm	392	675	APC850
Circular	0.2 mm	7mm diameter	0.25mm	441	507	APC850

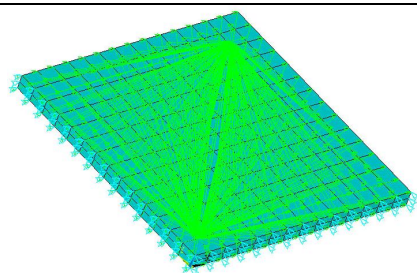


Figure 1 3-D mesh of square PWAS with boundary conditions

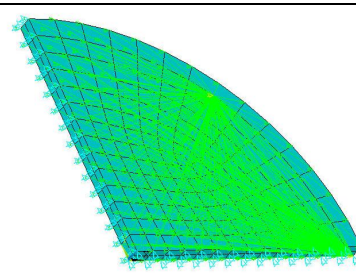


Figure 2 3-D mesh of circular PWAS with boundary conditions

The meshed squared PWAS is shown in Figure 1. The square is 7mm long, 7 mm wide and 0.2 mm thick. The circular PWAS has a diameter of 7mm and a thickness of 0.2mm. Only the top right quarter of the PAS was modeled to utilize the symmetry characteristic of the model. The PWAS was modeled using 3-D 8 nodes coupled field element that has 4 degrees of freedom at each node. This brick coupled field element is capable of modeling piezoelectric materials with its **VOLTAGE** degree of freedom activated. For the nodes at both the top and bottom surface, their **VOLTAGE** DOF were coupled to only one master node to simulate the electrode surface of the PWAS. It will also simplify the solution process and thus can yields a faster solution.

When a PWAS is excited either electrically or mechanically, resonance may happen when the response is very large. There could be of two types of resonance:

- Electromechanical resonances
- Mechanical resonances

Mechanical response takes place in the same condition as in a conventional elastic structure while electromechanical resonances are specific to piezoelectric materials⁸. Electromechanical resonances reflect the coupling between the mechanical and electrical variables, they happen under electric excitation, which produces electromechanical responses (i.e., both a mechanical vibration and a change in the electric admittance and impedance). When a PWAS is excited harmonically with a constant voltage at a given frequency, electrical resonance is associated with the situation in which a device is drawing very large currents. At resonance, the admittance becomes very large while the impedance goes to zero. As the admittance becomes very large, the current drawn under constant-voltage excitation also becomes very large because $I=Y \cdot U$. In piezoelectric devices, the mechanical response at electrical resonance also becomes very large. This happens because the electromechanical coupling of the piezoelectric materials transfers energy from the electrical input into the mechanical response.

To verify the result of the frequency response of PWAS E/M impedance, the simulation result was compared to the experimental data acquired with the HP 4194A Impedance Analyzer. The impedance measurements were done with 7 mm square PWAS ($l=7\text{mm}$, $b=7\text{mm}$, $t=0.2\text{mm}$, APC 850 Piezoceramic). The comparison was plotted in Figure 3 and Figure 4.

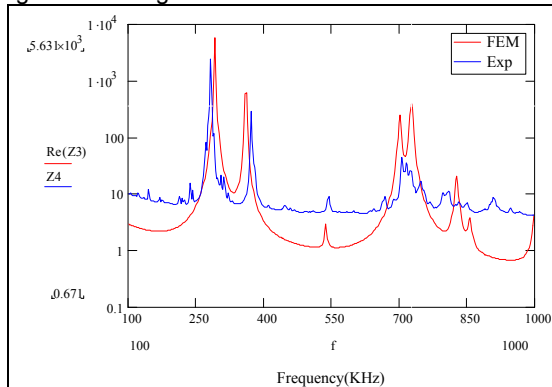


Figure 3 Comparison of real part frequency response of impedance of square PWAS between Simulated data and experimental result (100KHz-2MHz)

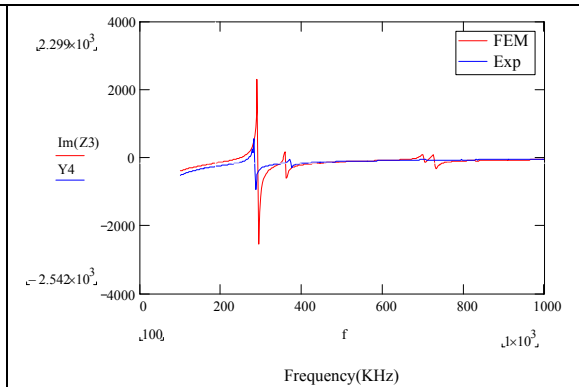


Figure 4 Comparison of imaginary part frequency response of impedance of square PWAS between Simulated data and experimental result (100KHz-2MHz)

From these comparisons we can see that the experimental results are in fairly good agreement with the simulated result especially for the relative low frequency range. The experimental curve shows an additional peak at around 920KHz and that may be due to the edge roughness generated during the manufacturing process.

We can continue our analysis on the circular PWAS with the same technique. The FE model of the circular PWAS, that has a diameter of 7mm and a thickness of 0,2mm, was shown in Figure 2.

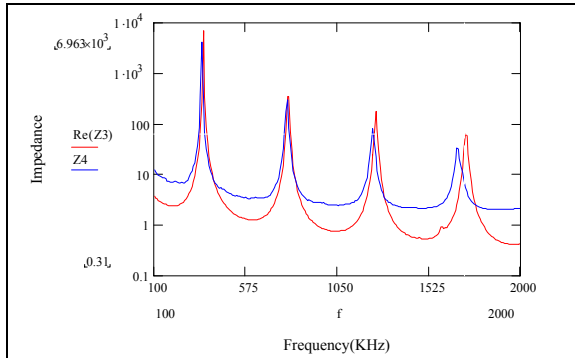


Figure 5 Comparison of real part frequency response of impedance of square PWAS between Simulated data and experimental result (100KHz-2MHz)

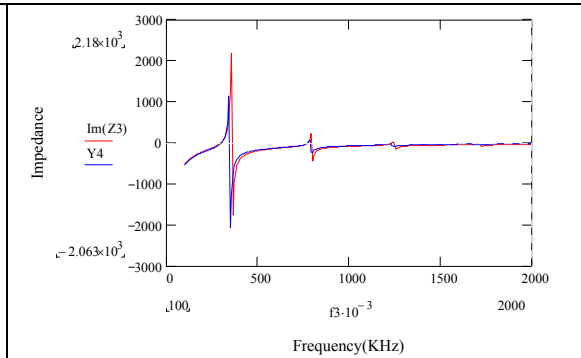


Figure 6 Comparison of real part frequency response of impedance of square PWAS between Simulated data and experimental result (100KHz-2MHz)

The simulated impedance data was then compared to the impedance measurements of circular PWAS and the comparison were given in Figure 5 and

Figure 6. These comparisons indicated a good agreement between finite element simulation and experiments. We can also see that in high frequency range (1500KHz-2000KHz), the simulated impedance peaks shifted a little from that of the experimental measurements, that may be explained that the element size and time step of harmonic analysis may not be appropriate at such high frequencies and thus can not yield the correct results. The effect of element size and time step at high frequencies will be explored in future work. According to previous discussion and comparisons, the overall conclusion could be made that good agreement between the FE simulation of E/M impedance of free PWAS and experimental data can be obtained with the coupled field analysis.

2.3. E/M impedance analysis of structure constrained PWAS

The previous chapter discussed the impedance simulation of free PWAS. This chapter will present the E/M impedance analysis of structures constrained PWAS. As stated in previous section, the electro-mechanical (E/M) impedance method uses in-plane surface excitation to measure the point wise mechanical impedance of the structure through the real part of the electrical impedance measured at the sensor terminals. The measured impedance parameters such as real and imaginary parts, amplitude, phase, etc. serve as potential indicators of structural damage. In this section we will first examine the analytical solution of the structure constrained PWAS E/M impedance; second pure structure FE analysis will be performed to infer the structure stiffness and then the PWAS impedance with the analytical equations. Finally we will model the structure and the PWAS with coupled field element to achieve a direct simulation of PWAS E/M impedance.

2.3.1. Analytical impedance analysis of 1-D beam with PWAS

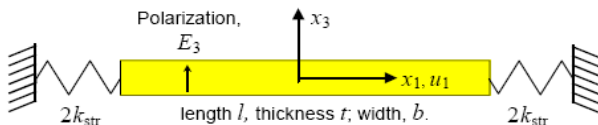


Figure 7 PZT wafer active sensor constrained by an overall structural stiffness, k_{str} . (Giurgiutiu and Zagari, 2000)⁹

Consider a constrained PZT active sensor of length l_a , thickness t_a and width b_a that undergoes longitudinal expansion (u_1) induced by the thickness polarization electric field as shown in Figure 7. The electric field ($E = V / t_a$) is produced by the application of a harmonic voltage ($V(t) = V e^{i\omega t}$) between the top and bottom surface (electrodes). When the PWAS is bonded to the structure, the structure will constrain the PWAS motion with a

structural stiffness k_{str} . The overall structural stiffness, k_{str} , has been split into two end components, each of size $2k_{str}$ for symmetry, Giurgiutiu and Zagari⁹ had given the admittance and impedance expressions for a PZT active sensor constrained by the structural substrate

$$Y = i\omega \cdot C \left[1 - \kappa_{31}^2 \left(1 - \frac{1}{\varphi \cot \varphi + r} \right) \right] \quad (1)$$

$$Z = \frac{1}{i\omega \cdot C} \left[1 - \kappa_{31}^2 \left(1 - \frac{1}{\varphi \cot \varphi + r} \right) \right]^{-1} \quad (2)$$

In that equation equivalent stiffness ratio $r = \frac{k_{str}}{r_{PZT}}$, C and κ_{31}^2 are PWAS related constants and φ are notation related to wave length and PWAS dimension.

2.3.2. PWAS E/M Impedance analysis of 1-D beam with FE structure simulation

One-dimensional beam structures are easy to model, and the prediction of their natural frequencies and vibration modes are fairly well understood¹⁰, so a natural idea is to instrument the beam with PWAS and study the dynamic characteristic of the beam through the frequency response of impedance. One further step will be to perform damage detection of the beam structure when cracks are created on it. From the above analytical discussion, we can see if we can find the structure stiffness, with the above equation, E/M impedance can be obtained. The structure stiffness k_{str} of the beam can be derived by calculating the response of structural substrate using the general theory of structural vibrations, thus the analytical solution of the E/M impedance of 1-D beam constrained PWAS can be obtained. We can also employ FEM to get the structure stiffness and calculate the impedance consequently. So, we will perform FE structure analysis on the structure to get the structure stiffness and then infer the E/M impedance.

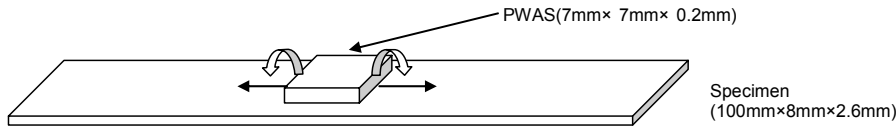


Figure 8 Structure layout of 1-D beam analysis

The 1-D beam model with PWAS is shown in Figure 8. The PWAS is installed at the location of 40 mm from left hand end with standard sensor-installation procedure. The size of the PWAS is almost the same as the height of the beam, so the movement in longitude direction dominates, thus simplify the analysis.

Table 2 1-D beam with square PWAS

Beam model					
	Thickness	Dimension	Number of elements	Number odes	Materials
Beam	2.6 mm	100mm × 8mm	98	128	Steel
Square PWAS	0.2 mm	7mm × 7mm	333	380	APC850

When the PWAS is excited, it will exert force and bending moment onto the beam. Figure 8 shows a PWAS affixed to the structural surface. The PWAS is directly connected to the source of electrical excitation through the connecting wires. The piezoelectric wafer is also intimately bonded to the structure, such that the strain/displacement compatibility and stress/force equilibrium principles apply. As the PZT material is activated electrically, strain is induced in the piezoelectric wafer, and interaction forces and moments appear at the interface between the sensor and the structure. In the pin-force model, the interaction force, F_{PZT} , is assumed to act at the sensor boundary only. Induced by F_{PZT} are activation forces and moments (N_a and M_a), which apply a pinching action to the structural surface and generate structural waves⁸.

$$F_{PZT} = |F_{PZT}| \cdot e^{i\omega t}, N_a = F_{PZT}, M_a = F_{PZT} \cdot \frac{h}{2} \quad (3)$$

The beam was modeled with shell element. As shown in Figure 8, harmonic excitation of force and moment were exerted at the borders of the PWAS to simulate the presence of the PWAS. The frequency response of the structure was then obtained through harmonic analysis.

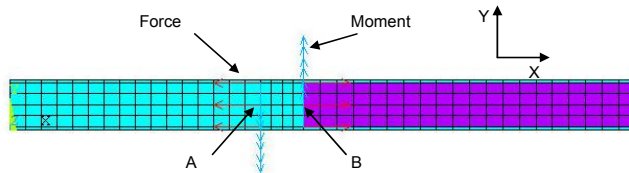


Figure 9 Meshed structure and applied loads of 1-D beam analysis

Two DOFs, translation displacement in X direction UX and rotation displacement in Y ROTY are used to calculate the structure frequency response function (FRF) when harmonic analysis at the frequency range from 10 KHz to 300 KHz was performed. The relative movement between the two edge points (A and B) was used to calculate the axial and flexural frequency responses function. Then overall structure stiffness was then obtained and substituted into the impedance and admittance equation.

Finally the FE derived impedance is compared to the analytical results and experimental results acquired with commercial impedance analyzer as shown in Figure 10. We can see that these results are in good agreement.

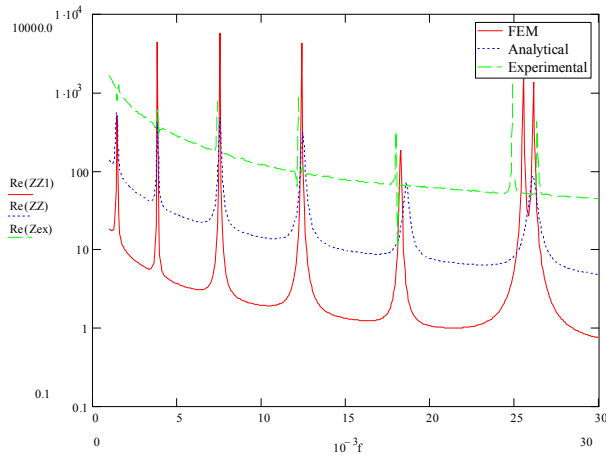


Figure 10 Comparison of the real part impedance of PWAS attached on the 1-D beam

2.4. Impedance analysis of 1-D beam with PWAS using coupled field finite element method

The next step is to simulate the 1-D beam structure and PWAS with coupled field element. With brick coupled field element, the direct interaction between mechanical motion and electrical potentials could be modeled in a nature way. As shown in Figure 11, the narrow beam and square PWAS were modeled with 3-d elements and the PWAS was bonded on the surface of the beam structure. Different materials properties, steel and piezoelectric material APC 850 were specified on the two objects modeled with different elements. The adjacent nodes between the beam and the PWAS were “glued” together in ANSYS, which means the strain and stress can be transferred from one of them to the other. Voltage DOFs were coupled for the nodes of the PWAS at both the top and bottom surface to simulate the electrodes. Harmonic analysis was performed to acquire the impedance data of the PWAS as done in the free PWAS analysis.

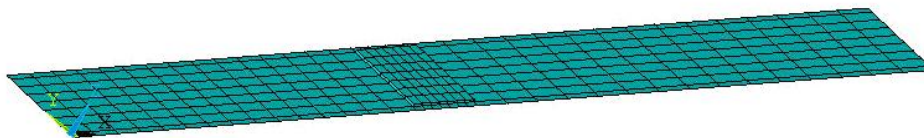


Figure 11 3-D mesh of narrow beam with PWAS

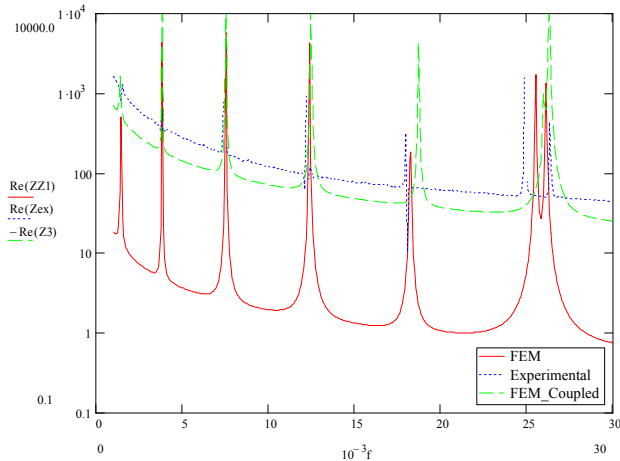


Figure 12 Comparison of real part of impedance to experimental data

Finally, the comparison plot of impedance real part between experimental result, non coupled field FE simulation and coupled field FE simulation was presented in Figure 12. From the comparison we can see that the impedance data obtained from the coupled field analysis was very closely to the experimental structure impedance data. These results validate the possibility of using the coupled field method to analyze and simulate the structure with piezoelectric sensors.

3. NUMERICAL SIMULATION OF WAVE PROPAGATION WITH PWAS

3.1. Introduction to Lamb wave

The study of wave propagation in an elastic medium has a long history. Elastic waves in solid media can travel in a variety of modes, each associated with a wave type: axial, shear, classical flexure, Rayleigh, Lamb, Love, etc.⁸. Elastic waves propagating in thin plates with free boundaries are called Lamb waves. Lamb waves are also known as guided plate waves, since the wave energy remains contained within the thin-plate guide. By using Lamb waves in a thin-wall structure, one can detect the existences and positions of cracks, corrosions, delaminations, and other damage¹¹. Wave propagation damage detection can be implemented in different methods, such as pitch catch, pulse echo and phase array. In the pitch-catch method, wave dispersion and attenuation due to diffused material-damage is used as a flaw indicator. In the pulse-echo method, defects are detected in the form of additional echoes. When an incident wave encounters a crack transverse to the wave propagation path, wave reflection may occur. This wave reflection may be sensed as an echo at the transmitter sensor (PWAS). The echo time of flight (TOF) is proportional with twice the distance between the transmitter sensor and the crack.

The Lamb wave particle displacements are both along the plate and across the thickness. Lamb waves can propagate in two modes, symmetric (S) and antisymmetric (A)⁸. The wave velocity depends on the product of frequency and material thickness. At low frequency the fundamental S0 and A0 Lamb modes approach the conventional axial and flexural plate waves.

3.2. Wave propagation simulation

In this section we will study the wave propagation in structures excited by PWAS. Our investigation was first focused on simple 1-D wave-propagation studies that allow a simpler analysis and foster rapid understanding. A narrow-strip aluminum beam (914mm long, 8 mm wide and 1.6 mm thick) as shown in Figure 13 was modeled using four-node shell element that has six degrees of freedom at each node. The shell element displayed both bending and membrane capabilities. The FEM also permitted the simulation of cracks through the thickness. Figure 14 shows a simulated crack placed transverse to the beam, along the transverse symmetry line. In order to obtain better resolution for crack simulation, the discretization mesh was locally refined, as indicated in Figure 14.

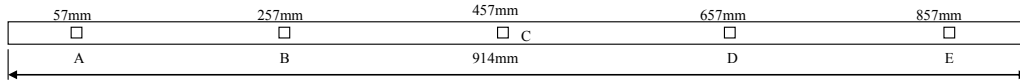


Figure 13 Narrow aluminum beam with PWAS sensors

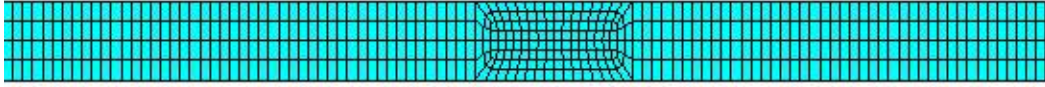


Figure 14 Mesh design of the beam and crack refinement (center part)

To model the wave excitation and reception process, we first define several groups of finite elements that cover certain areas on the beam to represent piezoelectric active sensor. The locations of these sensor areas were shown in Figure 13. We can then apply excitations on these equivalent sensor areas and examine the mechanical response acquired at simulated sensor areas. The positions of these sensors were shown in Figure 13.

The excitation signal considered in our studies consisted of a smoothed tone burst. The smoothed tone burst was obtained from a pure tone burst of frequency f filtered through a Hanning window. The Hanning window was described by the equation:

$$x(t) = \frac{1}{2} [1 - \cos(2\pi t/T_H)], t \in [0, T_H] \quad (4)$$

The number of counts, N_B , in the tone bursts matches the length of the Hanning window, i.e., $T_H = N_B/f$ (5)

The tone burst excitation was chosen in order to excite coherent single-frequency waves. This aspect is very important especially when dealing with dispersive waves (flexure, Rayleigh, Lamb, Love, etc). The Hanning window smoothing was applied to reduce the excitation of frequency side lobes associated with the sharp transition at the start and the end of a conventional tone burst.

Two forms of the elastic wave propagation were studied: the axial waves and the flexural waves. We applied function-generated load of force and moment to the nodes delimiting the contour of these active areas. Consistent with the physical phenomenon, the force applied to nodes representing opposite ends of the piezoelectric wafer had to be in opposite phase. This ensures that the net effect on the structure is self-equilibrating. To generate axial waves, we applied force on the nodes. While for flexural waves, we applied moments. The detection of the elastic waves followed the same general principle as that applied to wave generation. The variables of interest were the differences between the displacements at the opposing ends of the active sensor, i.e., delta displacement for axial waves, and delta rotation for flexural waves.

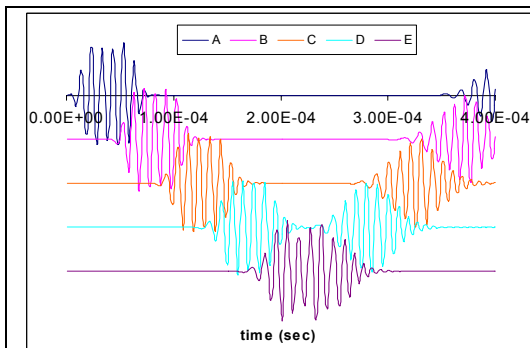


Figure 15 FEM simulation of the axial wave signals received at sensor A-E (100KHz five count smoothed tone-burst excitation at active sensor A)

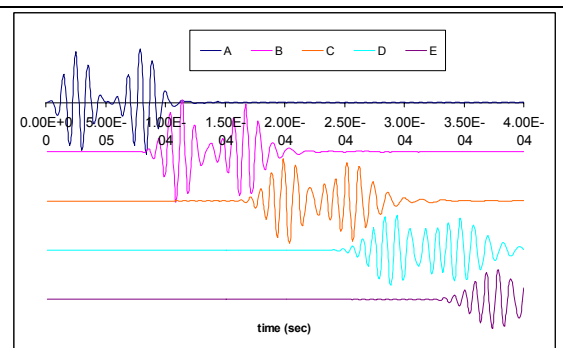


Figure 16 FEM simulation of the flexural wave signals received at sensor A-E (100KHz five count smoothed tone-burst excitation at active sensor A)

Figure 15 shows FEM simulation of axial waves signal received at sensors A–E when the beam was excited with a 100 kHz five-count Hanning-windowed axial burst at the left-hand end of the beam. It is easily appreciated how the wave travels down the beam from A to E, then reflects at the right-hand end, and returns to A, followed by repetition of this pattern. We observe that, at the beginning, the five counts of the smoothed tone-burst excitation can be readily identified. As the wave travels further and undergoes reflections, its coherence somehow diminishes, and

some dispersion occurs. This loss of coherence may also be attributed to accumulation of numerical error. Flexural wave was also simulated with a 100 KHz five-count Hanning-windowed axial burst at the left-hand end as shown in Figure 16. We note that the two burst wave packages were apparent in the wave form and that's due to the reflection of the incident wave at the left-hand end of the beam. We observe that the flexural wave speed is roughly half of that of axial wave, since for the same distance; the flexural took roughly twice the traveling time.

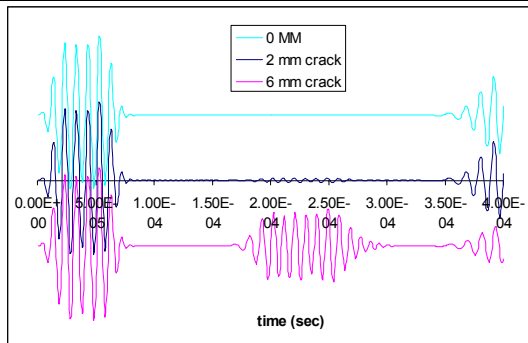


Figure 17 FEM simulation of pulse echo method in narrow beam using axial waves

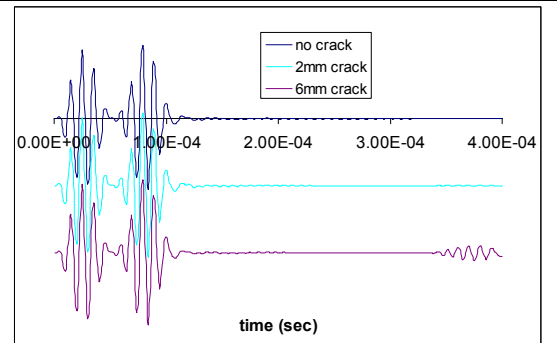


Figure 18 FEM simulation of pulse echo method in narrow beam using flexural waves

Figure 17 shows the FEM simulation of the pulse-echo method used for crack detection. The active sensor placed at the left-hand end was used to send a 100 kHz five-count Hanning-windowed axial burst and to receive the elastic wave responses. Three situations: no crack, 2 mm crack and 6 mm crack were presented. In a beam without crack, the initial signal and the reflection from the right-hand end appear. If a 2 mm through-the-thickness transverse crack is simulated in the center of the beam, the reflection (echo) from this crack also appears but the amplitude of reflection was quite small, when the crack length increases from 2 mm to 6 mm, the amplitude of the reflection increases significantly.

Figure 18 shows the FEM simulation of the pulse-echo method used for crack detection with flexural wave. Three situations: no crack, 2 mm crack and 6 mm crack were presented. In a beam without crack, the initial signal and the reflection from the right-hand end appear. We could observe similar result as in the case of axial wave.

3.3. Coupled field wave propagation simulation

In previous analysis, waves were generated by applying force or moments on the beam, thus different modes of wave were separated and in some sense the real complex situation of wave composition and interaction were simplified, another issue is that the way to sense the wave motion, in the simulations we just discussed, pure structure response like relative displacement and rotation were used to analyze the structure response, while the piezoelectric effect of PWAS were not taken in account.

To solve these issues, we will apply the coupled analysis on the structure, i.e., we will model PWAS directly with coupled field elements, excite the PWAS with electrical signals and examine the electrical response of PWAS to the wave motion. The specimen we examined was shown in Figure 19. Five PWAS sensors were bonded on the aluminum beam. In our FEM model, the PWAS model were constructed with solid elements and attached on the solid beam model. Part of the FEM model was shown in Figure 20. Bottom surface of the solid PWAS model was connected to the beam surface and thus mechanical motion will be transferred between the two models. A similar 100 kHz three-count tone burst signal was used to excite the structure. The difference here is that the excitation signals this time will be electrical voltage directly fed onto the top surface of the PWAS, simulating the operation as in real applications.

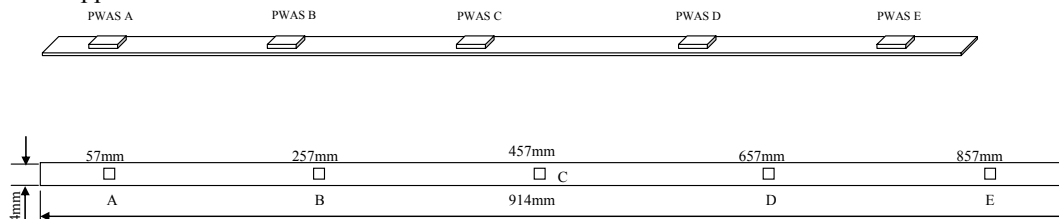


Figure 19 Mesh design of the beam and PWAS model

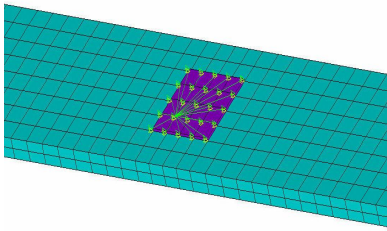


Figure 20 Mesh design of the beam and PWAS model

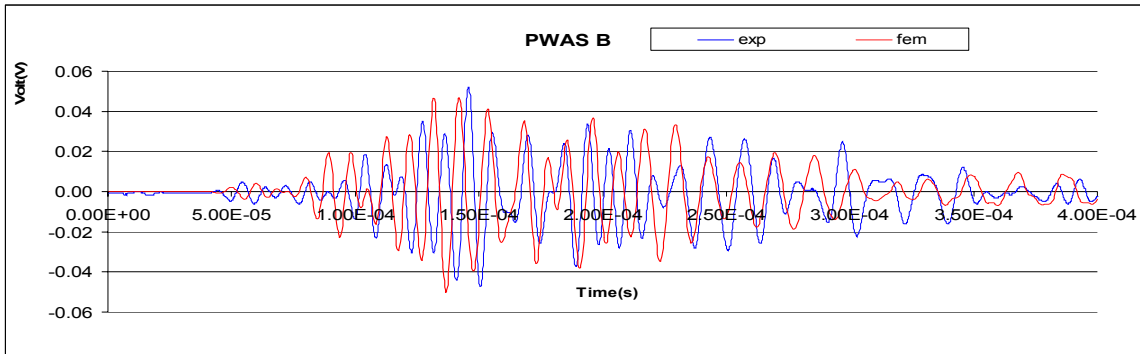


Figure 21 FEM simulation of electrical signal examined at PWAS C

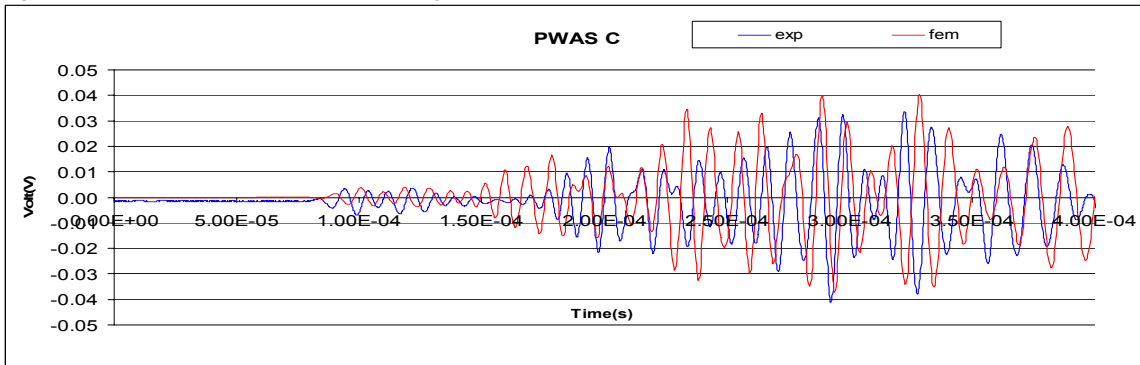


Figure 22 FEM simulation of electrical signal examined at PWAS D

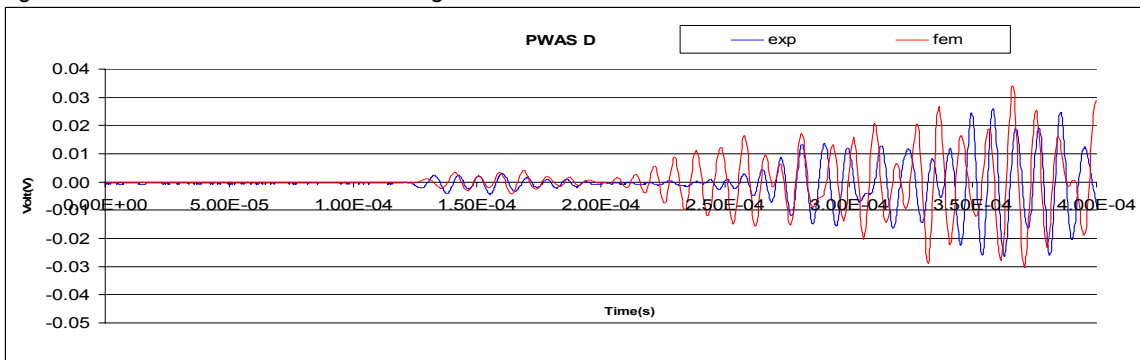


Figure 23 FEM simulation of electrical signal examined at PWAS E

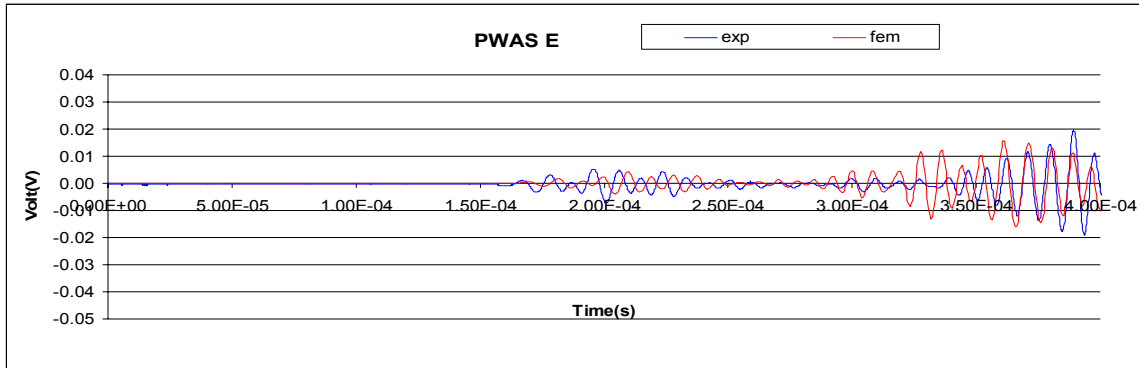


Figure 24 FEM simulation of electrical signal examined at PWAS B

The simulation results of electrical signals as well as experimental results examined at PWAS were presented in Figure 21 to Figure 24. We could observe that because when the PWAS was excited by electrical signals, the generated wave will incorporate both axial mode and flexural mode, also due to the reflection from the boundaries, thus the wave packet are more complex than the previous mechanical excitation situation. In the future work we try to tune the excitation and modify the models so that we can examine simpler and clearer wave mode.

4. CONCLUSION

Numerical simulations should be combined with both analytical analysis and practical experiments to optimize the study and applications of PWAS based SHM. In this paper we investigate the possibility of using FEM to study SHM techniques with PWAS. Both E/M impedance technique and wave propagation methods are studied. In this paper we showed that coupled field elements and analysis could be a power tool in simulating the PWAS based SHM methods.

For the simulation of the E/M impedance technique, impedance of free PWAS (square and circular) were simulated with coupled field elements followed by the impedance simulation of structure constrained PWAS. Close match of simulated result to the experimental data were illustrated. The future work could be continued on the impedance simulation on cracks situations and under different boundary conditions.

The wave propagation method of SHM is also investigated. Theory of guided wave was introduced, when PWAS is excited with alternating electrical signals, guided Lamb wave could be generated and propagate along the structure. At low frequency the fundamental S₀ and A₀ Lamb modes approach the conventional axial and flexural plate waves.

Finite element analysis of axial wave and flexural traveling in a narrow beam were performed; different size of cracks on the transverse symmetry line were simulated and reflection wave from the cracks can be identified in the wave plots. The motion excited by PWAS on the structure was simulated by axial forces and moments exerted on the borders of elements groups simulating the existence of PWAS. In addition, we apply the coupled field method to simulate wave propagation problem. PWAS were modeled with coupled elements and they were excited by electrical signals.

ACKNOWLEDGMENTS

This material is based upon work supported by the National Science Foundation under Grant # CMS-0408578 and CMS-0528873, Dr. Shih Chi Liu Program Director and by the Air Force Office of Scientific Research under Grant # FA9550-04-0085, Capt. Clark Allred, PhD Program Manager. Any opinions, findings, and conclusions or recommendations expressed in this material are those of the authors and do not necessarily reflect the views of the National Science Foundation or the Air Force Office of Scientific Research.

REFERENCES

1. Giurgiutiu, V., 2003, "Embedded NDE with Piezoelectric Wafer Active Sensors in Aerospace Applications," *Journal of Materials (JOM-e)*, Special Issue on NDE, Vol. 55, No. 1.
2. Jan Soderkvist, "Using FEA To Treat Piezoelectric Low-frequency Resonators", *IEEE transactions on ultrasonics, terroelectrics, and frrequency control*, Vol 45 No 3, May 1998
3. Park, G., Cudney, H., and Inman, D.J., 2000b, "An Integrated Health Monitoring Technique Using Structural Impedance

- Sensors,” *Journal of Intelligent Material Systems and Structures*, Vol. 11, No. 6, 448–455
- Rose, J.L. 1999. *Ultrasonic Waves in Solid Media*, Cambridge University Press, New York.
4. Liang, C., F. P. SUN, and C. A. ROGERS (1993) "An Impedance Method for Dynamic Analysis of Active Material Systems, Proceedings, 34th AIAA/ASME/ASCE/AHS/ASC SDM Conference, La Jolla, CA, 19-21 April 1993; pp. 3587-3599
 5. SUN, F. P., Z. CHAUDHRY, C. LIANG, and C. A. ROGERS (1995). "Truss Structure Integrity Identification Using PZT Sensor-Actuator," *Journal of Intelligent Material Systems and Structures*, Vol. 6, No. 1, pp. 134-139
 - Giurgiutiu, V., Reynolds, A.N., and Rogers, C.A., 1999, "Experimental Investigation of E/M Impedance Health Monitoring of Spot-Welded Structural Joints," *Journal of Intelligent Material Systems and Structures*, Vol. 10, 802–812.
 6. Giurgiutiu, V., and Rogers, C. A. 1997, "Electro-mechanical (E/M) impedance method for structural health monitoring and non-destructive evaluation", *International Workshop on Structural Health Monitoring*, Stanford University, CA, September 18-20, 1997, pp. 433-444
 7. Giurgiutiu, V., and Zagrai, A. N., 2002, "Embedded Self-Sensing Piezoelectric Active Sensors for Online Structural Identification," *ASME Journal of Vibration and Acoustics*, Vol. 124, 116–125
 8. Giurgiutiu, V.; Lyshevski, S. E. (2004), *Micromechatronics Modeling, Analysis, and Design with MATLAB*, CRC Press, 2004
 9. Giurgiutiu, V., and Zagrai, A., 2000, "Characterization of Piezoelectric Wafer Active Sensors," *Journal of Intelligent Material Systems and Structures*, Vol. 11, 959–976.
 10. Inman, D. J., (1996) "Engineering Vibration", Prentice-Hall, Inc., 1996.
 11. Rose, J.L. 2001. "A Vision of Ultrasonic Guided Wave Inspection Potential," In: *Proceeding of the 7th ASME NDE Topical Conference*, NDE-Vol. 20, pp. 1–5.